

# Modulation of effector affinity by hinge region mutations also modulates switching activity in an engineered allosteric TEM1 $\beta$ -lactamase switch

Jin Ryoung Kim, Marc Ostermeier \*

Department of Chemical and Biomolecular Engineering, Johns Hopkins University, 3400 N. Charles Street, Baltimore, MD 21218, USA

Received 10 October 2005, and in revised form 21 November 2005

Available online 9 December 2005

## Abstract

RG13 is an engineered allosteric  $\beta$ -lactamase (BLA) for which maltose is a positive effector. RG13 is a hybrid protein between TEM1 BLA and maltose-binding protein (MBP). Maltose binding to MBP is known to convert the open form of the protein to the closed form through conformational changes about the hinge region. We have constructed and genetically selected several variants of RG13 modified in the hinge region of the MBP domain and explored their effect on  $\beta$ -lactam hydrolysis, maltose affinity and maltose-induced switching. Hinge mutations that increased maltose affinity the most (and thus presumably close the apo-MBP domain the most) also abrogated switching the most. We provide evidence for a model of RG13 switching in which there exists a threshold conformation between the open to closed form of the MBP domain that divides states that catalyze  $\beta$ -lactam hydrolysis with different relative rates of acylation and deacylation.

© 2005 Elsevier Inc. All rights reserved.

**Keywords:**  $\beta$ -lactamase; Maltose-binding protein; Allostery; Switch

Enzymes whose activity is modulated by an analyte can be used as molecular sensors for the detection of that analyte. It is thus an important goal of biotechnology to create enzymes whose activity is modulated by analytes of our choosing. One approach for detecting protein analytes is to replace surface loops of an enzyme with an antibody epitope such that antibody binding to this epitope modulates enzyme activity [1,2]. For example, the phage display of a TEM1  $\beta$ -lactamase (BLA)<sup>1</sup> library with randomized surface loops has been applied to identify a BLA variant that is regulated by a monoclonal antibody against the prostate-specific antigen and thus useful as a signaling molecule for the detection of the prostate-specific antigen in a competitive assay [3]. An alternate strategy is to directly couple the analyte detecting domain and the enzyme activity by gene

fusion, but the challenge is how to combine two proteins in a manner that couples their functions.

Recently, a handful of studies have shown how domain insertion can be used to couple two proteins' functions [4]. For example, domain insertion was used to engineer an allosteric  $\beta$ -lactamase (RG13) for which maltose is a positive, heterotropic effector [5]. RG13 was identified from a combinatorial library in which randomly circularly permuted variants of the gene coding for BLA were randomly inserted into the gene for *Escherichia coli* maltose-binding protein (MBP). In RG13, the original N- and C-termini of BLA are joined by a GSGGG peptide linker, and the BLA domain is circularly permuted between residues 226 and 227. This circularly permuted variant is inserted into MBP in place of MBP residue 317. In the presence of saturating concentrations of maltose, RG13 has kinetic parameters for nitrocefin (NCF) hydrolysis that are essentially the same as BLA. In the absence of maltose, the kinetic properties are compromised ( $k_{\text{cat}}$  is threefold lower and  $K_m$  is eightfold higher). The dissociation constant ( $K_d$ )

\* Corresponding author. Fax: +1 410 516 5510.

E-mail address: [oster@jhu.edu](mailto:oster@jhu.edu) (M. Ostermeier).

<sup>1</sup> Abbreviations used: BLA,  $\beta$ -lactamase; MBP, maltose-binding protein; NCF, nitrocefin; CFTX, cefotaxime.

of RG13 and maltose is 5 mM in the absence of substrate. The  $K_d$  for maltose in the presence of saturating amounts of the BLA substrate carbenicillin is fivefold lower, indicating that maltose binding and substrate binding are coupled functions. Thus, maltose binding modulates the catalytic properties of RG13 by affecting substrate binding and the rates of the chemical steps. Recently, BLA–MBP switches with even larger changes in activity upon maltose binding have been created [6]. These switches consist of different circular permutations of BLA inserted in place of MBP residue 317.

Maltose-binding protein exists as a single polypeptide chain protein with two globular domains connected by a hinge region [7]. This hinge region is comprised of a two-stranded  $\beta$ -sheet and a short  $\alpha$ -helix (positions 305–313). A conformational change (a  $35^\circ$  bending) occurs about this hinge upon maltose binding, converting the protein from the ligand-free open conformation to a ligand-bound closed conformation (Fig. 1). The maltose-binding pocket is at the interface of the two domains in the vicinity of several tryptophan residues. Maltose binding occurs with  $\sim 10\%$  quenching in the intrinsic fluorescence and a small wavelength shift [9]. RG13 exhibits a similar fluorescent quenching and wavelength shift in the presence of maltose, suggesting that the MBP domain in RG13 undergoes a similar conformational change [5]. The coincidence of fluorescent quenching and changes in catalytic activity implicate the conformational change in the modulation of enzymatic activity.

Further evidence for the role of the conformational change came from characterizing I329W and I329W/A96W mutants in the hinge region of the MBP domain of RG13. Marvin and Hellinga [10] designed these mutations in MBP to manipulate the conformational equilibria between the open and the closed state. The apo forms of these mutants are partially closed relative to the apo wild-type MBP with the ensemble average closure angles being  $9.5^\circ$  and  $28.4^\circ$  for I329W and I329W/A96W, respectively [11]. The ligand-bound closed forms of MBP, MBP(I329W) and MBP(I329W/A96W), have closure angles of  $35^\circ$ . Partial closing shifts the equilibrium toward the ligand-bound state and thus the mutations increase the affinity for maltose. Introduction of these mutations into RG13 created variants with increased affinity for maltose and with BLA activity that could be modulated with lower concentrations of maltose [5]. However, the switching was significantly diminished for RG13(I329W/A96W) i.e., the variant with mutations that close the apo-form of MBP the furthest. A decrease in switching could result from the mutations raising the BLA activity in the absence of maltose, lowering the activity in the presence of maltose, or both. In the case of RG13(I329W/A96W), switching was abrogated solely by raising the BLA activity of the switch in the absence of maltose [5]. This suggests that it takes hinge bending angle between  $9.5^\circ$  and  $28.4^\circ$  to alleviate the defect in RG13 BLA activity in the absence of maltose. However, the closure angles of RG13 or the variants are not known.

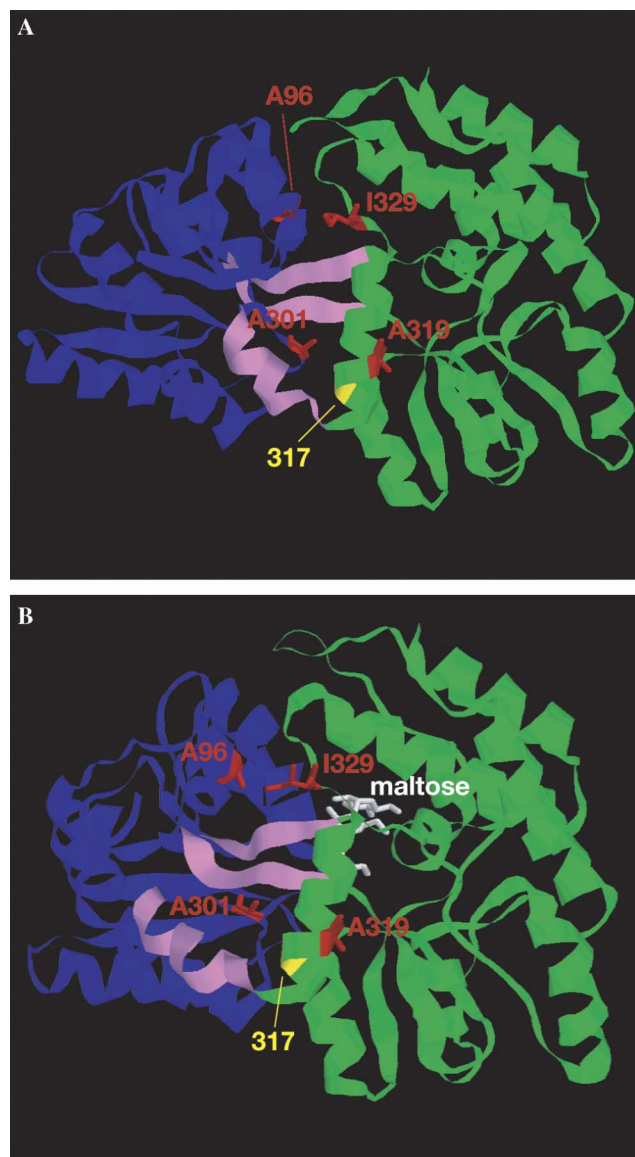


Fig. 1. Ribbon diagrams of the structure of maltose-binding protein (MBP). (A) Apo open-form (1OMP) [7] and (B) maltose-bound closed form of MBP (3MBP) [8]. The two globular domains are shown in blue and green and the two  $\beta$ -sheets and one  $\alpha$ -helix that span the hinge region are shown in pink. Four amino acid residues (A96, I329, A301, and A319) located in hinge region of MBP or its vicinity are shown in red. The site of insertion of BLA into MBP in RG13 is shown in yellow. Maltose is shown in white. Amino acid numbers correspond to that of MBP and not RG13.

Substitutions of a variety of natural and non-natural side chains at position I329 in MBP suggested that the dominant determinants of the equilibria between the open and closed states are differences in steric complementarity of the mutant side chain and its local surroundings in the open and closed states [10,11]. Here, we have constructed several natural amino acid variants at position I329 in RG13 and explored their effect on RG13-catalyzed  $\beta$ -lactam hydrolysis, maltose affinity, and maltose-induced switching. These studies are consistent with the view that I329 mutations that increase maltose affinity the most (and thus presumably close the apo-MBP domain the

most) also abrogate switching the most. In addition, we identified through genetic selection, two mutations in the MBP domain of RG13 (A301T and A319T) that are at or near the hinge region that also serve to increase maltose affinity as well as decrease switching activity. Finally, we provide evidence that for NCF hydrolysis catalyzed by RG13 in the absence of maltose, the rate of deacylation is less than or comparable to the rate of acylation. In contrast, in the presence of maltose the rate of deacylation is much greater than the rate of acylation. This provides evidence for a model of RG13 switching in which conformational changes that occur part way through the hinge bending motion in the MBP domain (from open to closed) switch the BLA domain from a state with low deacylation rates to one with high deacylation rates.

## Materials and methods

### Materials

Qiaquick PCR purification kit and Qiaquick gel extraction kit were purchased from Qiagen (Valencia, CA, USA). His-tag protein purification kit was purchased from Novagen (Madison, WI, USA). *Taq* polymerase was purchased from Promega (Madison, WI, USA). Oligonucleotides and Electromax DH5 $\alpha$ -E electrocompetent cells were purchased from Invitrogen (Carlsbad, CA, USA). NCF was purchased from Remel (Lenexa, KS, USA). Cefotaxime (CFTX) was purchased from Sigma (St. Louis, MO, USA). All other antibiotics and maltose were purchased from Fisher Scientific (Pittsburgh, PA, USA).

### Mutagenesis at 329 position

All designed mutations described were introduced into pET24b-RG13 [5] by Quickchange mutagenesis. Desired mutations were confirmed by DNA sequencing.

### Protein expression and purification

One liter LB media containing 50  $\mu$ g/mL kanamycin was inoculated with 2% overnight culture and shaken at 37 °C. Cells were grown at 37 °C until the OD<sub>600 nm</sub> was 0.5. IPTG was added to 1 mM and the culture was shaken at 22 °C for another 6 h. Cells were pelleted and resuspended in binding buffer supplied by the His-tag protein purification kit and lysed by French press. The soluble fraction was recovered and passed over the Ni<sup>2+</sup> column. The protein was eluted with 120 mM imidazole solution and dialyzed at 4 °C against 3 L of 100 mM sodium chloride, 50 mM sodium phosphate buffer overnight followed by dialysis against 1 L of the same buffer containing 20% glycerol for 6 h. Protein was stored in aliquots at –80 °C. The purities of the proteins were estimated by Coomassie Blue staining of SDS-PAGE gels and were greater than 95%, unless otherwise described. Protein concentrations were determined using extinction coefficients at 280 nm as described [12].

### Steady-state kinetics

All kinetic assays were performed with  $\sim$ 4 nM protein at 25 °C in 100 mM sodium phosphate buffer, pH 7.0. Enzyme was incubated at 25 °C for 1 min in sodium phosphate buffer with or without 5 mM maltose prior to addition of substrates. During NCF hydrolysis, absorbance at 486 nm was recorded over time and the kinetic parameters were determined from the initial rate of reaction using Eadie–Hofstee plots. In the absence of maltose, NCF hydrolysis catalyzed by RG13 and all mutants exhibited a slight initial lag that was more pronounced at high NCF concentration, as described previously [5], and the kinetic parameters were determined by measuring the rate after the lag. NCF concentration was corrected by subtracting the amount of hydrolyzed NCF. In all cases, the extent of reaction at the point the rate was measured was less than 5%. No lag was observed in the presence of maltose. The rate of hydrolysis of 100  $\mu$ M NCF in the presence of hydroxylamine was measured in the same way as above except for the addition of hydroxylamine to the assay buffer. The rates were corrected by subtracting the rate of NCF hydrolysis by hydroxylamine alone. For CFTX hydrolysis, absorbance at 260 nm was monitored as a function of time. Direct evaluation of kinetic parameters from initial rates was not possible due to the slow hydrolysis rate and large absorbance at 260 nm at concentrations of CFTX much less than  $K_{m,CFTX}$ . Therefore,  $K_m$  was determined using a competitive assay with 100  $\mu$ M NCF as described elsewhere [13]. The value of  $k_{cat}/K_m$  was determined from steady-state rates with 80  $\mu$ M of CFTX. No lag was observed in CFTX hydrolysis even in the absence of maltose.

### Maltose affinity and fluorescence quenching by maltose

Dissociation constants ( $K_d$ ) for maltose were determined using intrinsic tryptophan fluorescence measured on a Photon Technology QuantaMaster QM-4 spectrofluorometer. The protein concentration was  $\sim$ 50 nM. Excitation was at 280 nm and the quenching extent of fluorescence intensity at 341 nm upon addition of maltose was used to determine  $K_d$  using Eadie–Hofstee equivalent plots. For the I329D and I329H mutants, which showed insufficient fluorescence quenching to accurately determine  $K_d$ , the apparent dissociation constant in the presence of sub-saturating concentration of NCF (25  $\mu$ M) was determined by measuring the initial rate of NCF hydrolysis as a function of maltose concentration.

### Construction of random mutagenesis library of RG13

A random mutagenesis library was constructed from pDIM-C8-RG13 [5] using error-prone PCR with *Taq* polymerase with 5'-CTGTTCCGCTGGGCATGC-3' as the forward primer and 5'-CCGGTCTGAATGCATAAGCTTACTAACTAGT-3' as the reverse primer. The concentration of MnCl<sub>2</sub> was adjusted to 1 mM so that, on average, one

amino acid change was incorporated per library member. The desired PCR products were purified by Qiaquick PCR purification kit, digested by *SpeI* and *SphI*, and purified again. Plasmid pDIM-C8-MalE [14] was digested with *SpeI* and *SphI* and purified by Qiaquick gel extraction kit. PCR products were ligated to cut pDIM-C8-MalE plasmid. After ethanol precipitation, 20% of the ligation product was electroporated into 40  $\mu$ L Electromax DH5 $\alpha$ -E. Electroporated cells were plated on a large (248 mm  $\times$  248 mm) LB agar plate supplemented with 50  $\mu$ g/mL chloramphenicol. The naïve library was recovered from the large plate and stored in frozen aliquots as described [15].

### Library selection and screening

The naïve library was plated on LB agar plates supplemented with 256  $\mu$ g/mL ampicillin and 50  $\mu$ g/mL chloramphenicol and incubated at 37 °C overnight. From these plates, 384 colonies were picked to inoculate 1 mL LB media (supplemented with 50  $\mu$ g/mL chloramphenicol and 1 mM IPTG) in 96-well format. After incubation for 3 h at 37 °C followed by 25 °C overnight, each culture was lysed using 50  $\mu$ L PopCulture reagent, 40 units of rLysozyme, and 2.5 units of benzonase nuclease. Lysates were centrifuged to pellet the insoluble material and the soluble fractions were assayed in 96-well format for NCF hydrolysis in the presence and absence of 5 mM maltose and absorbance changes at 486 nm over time were recorded. The assays were carried out at room temperature using the Spectramax-384 Plus microplate reader (Molecular Devices) in the presence of 100 mM sodium phosphate buffer and 50  $\mu$ M NCF in a 200  $\mu$ L reaction volume. Clones whose lysates exhibited a less than threefold increase in the rate of NCF hydrolysis in the presence of maltose compared to its absence were recultured and their plasmids were sequenced. Two separate mutations, A301T and A319T, were identified. These two mutations were introduced into pET24b-RG13 by Quickchange mutagenesis. The proteins were expressed and purified as above.

### Ethyl acetate extraction

One hundred micromolar NCF was reacted with 0.5–1.2  $\mu$ M RG13 in the presence and absence of 40 mM hydroxylamine in the assay buffer containing either 5 mM or no maltose. After the reaction was complete, 2 mL of reaction mixture was extracted with 10 mL of ethyl acetate twice. The concentration of product in the ethyl acetate-rich phase was determined by absorbance at 486 nm. The molar extinction coefficient at 486 nm of hydroxylamine-modified NCF was identical to that of hydrolyzed NCF.

## Results and discussion

We investigated the effects of I329 mutations on the switching activity and maltose affinity of RG13. We have previously characterized the effect of a large aromatic substi-

tion (I329W) on these properties [5]. Here, eight new variants with a mutation at I329 were constructed. The amino acids for these mutations were chosen to sample a wide range of properties: small aliphatic (A), negatively charged polar (D), positively charge polar (K, R, H), uncharged polar (S, N), and cyclic (P). All mutants (and RG13) have a C-terminal His-tag for purification purposes. Three of the eight mutants (I329R, I329N, and I329S) could not be purified sufficiently (purity was <10%). Thus, detailed characterization of these mutants was not performed. However, the other five mutants (I329A, I329D, I329K, I329H, and I329P) were purified to >95% purity and retained BLA activity, maltose affinity, and switching activity.

### Effect of I329 mutations on maltose-binding affinity

We determined the  $K_d$  of RG13 and the mutants for maltose in the absence of substrate. The  $K_d$ 's of I329A, I329K, I329P, I329W, and RG13 were determined using quenching of intrinsic protein fluorescence upon maltose binding as a signal [9]. Due to the low level of fluorescent quenching observed with I329D and I329H, apparent  $K_d$ 's were measured instead using maltose's effect on NCF hydrolysis [5]. The  $K_d$ 's varied from  $\sim$ 25 nM to  $\sim$ 25  $\mu$ M depending on the amino acid at position 329 (Table 1 and Fig. 2). Those mutants with the greatest affinity for maltose (I329D and I329H) also had the lowest fluorescent quenching, consistent with the view that I329 mutations in MBP that close the apo form of the protein the most exhibited stronger affinity for maltose [10,11]. The affinity of I329H for maltose was  $\sim$ 200-fold greater than that of RG13. The magnitude of the effect of the I329H mutation on affinity for maltose in RG13 was larger than that observed with other natural substitution at I329 in MBP and comparable to that of non-natural amino acid substitutions that increased affinity the most [10].

### Effect of I329 mutations on catalytic and switching activity

The three mutants that could not be purified sufficiently (I329N, I329R, and I329S) had compromised BLA activity ( $k_{cat}/K_m$  for NCF was estimated to be <5% of that of RG13) that was independent of maltose (data not shown). However, the five other mutants retained substantial  $\beta$ -lactam hydrolysis activity as indicated by their catalytic parameters for the hydrolysis of NCF (Table 1) and CFTX (Table 2). Although all five retained at least partial switching activity, those mutants with the highest affinity for maltose (I329H and I329D) had the lowest switching (Figs. 2B and C). For I329H and I329D, the switching activity that remained primarily derived from the effect of maltose on  $k_{cat}$  and not on  $K_m$ . The lack of effect of maltose on  $K_m$  resulted from the mutation alleviating the defect in  $K_m$  observed in RG13 in the absence of maltose. The relationship between maltose affinity, switching activity, and the catalytic parameters observed in the I329D and I329H mutants was also seen in the previously characterized I329W/A96W double

Table 1  
Kinetic parameters of nitrocefin (NCF) hydrolysis of RG13 and mutants in the presence and absence of maltose

	RG13 <sup>a</sup>	I329W <sup>a</sup>	I329P	I329A	I329D	I329K	I329H <sup>b</sup>
$k_{\text{cat,mal}}$ (s <sup>-1</sup> )	620 ± 60	620 ± 60	550 ± 60	390 ± 50	210 ± 20	380 ± 50	410 ± 70
$k_{\text{cat,0}}$ (s <sup>-1</sup> )	200 ± 40	200 ± 30	140 ± 20	120 ± 20	70 ± 10	50 ± 20	120 ± 20
$k_{\text{cat,mal}}/k_{\text{cat,0}}$	3.1 ± 0.7	3.1 ± 0.6	4.0 ± 0.3	3.3 ± 0.4	3.0 ± 0.4	7.6 ± 3.1	3.4 ± 0.7
$K_{\text{m,mal}}$ (μM)	68 ± 4	53 ± 7	120 ± 20	60 ± 8	48 ± 2	60 ± 14	80 ± 20
$K_{\text{m,0}}$ (μM)	550 ± 120	350 ± 60	330 ± 40	350 ± 50	60 ± 10	240 ± 80	50 ± 20
$K_{\text{m,0}}/K_{\text{m,mal}}$	8.1 ± 2.0	6.6 ± 1.4	2.8 ± 0.6	5.8 ± 1.1	1.3 ± 0.2	4.0 ± 1.6	0.6 ± 0.3
$k_{\text{cat,mal}}/K_{\text{m,mal}}$ (s <sup>-1</sup> μM <sup>-1</sup> )	9.1 ± 1.0	11.7 ± 1.9	4.6 ± 0.9	7.0 ± 1.2	4.4 ± 0.5	6.3 ± 1.7	5.1 ± 1.5
$k_{\text{cat,0}}/K_{\text{m,0}}$ (s <sup>-1</sup> μM <sup>-1</sup> )	0.4 ± 0.1	0.6 ± 0.1	0.4 ± 0.1	0.3 ± 0.1	1.1 ± 0.3	0.2 ± 0.1	2.4 ± 1.0
$(k_{\text{cat,mal}}/K_{\text{m,mal}})/(k_{\text{cat,0}}/K_{\text{m,0}})$	25 ± 6	20 ± 5	12 ± 2	23 ± 5	4 ± 0.8	32 ± 18	2 ± 1
$K_{\text{d}}$ for maltose (μM)	5.5 ± 0.5	0.55 ± 0.13	25.6 ± 5.8	0.67 ± 0.15	0.38 ± 0.04	0.63 ± 0.015	0.025 ± 0.001

Subscript ‘mal’ and ‘0’ represent assay conditions in the presence of 5 mM maltose and absence of maltose, respectively.

<sup>a</sup> From Guntas et al. [5].

<sup>b</sup> I329H showed complex kinetics including an initial burst and apparent substrate inhibition at  $\geq 200$  μM NCF but followed Michaelis–Menten kinetics at  $< 200$  μM.

mutant [5]. Structural information on RG13 would be very useful in deciphering mechanism underlying the switch, but it is not available. However, the fact that RG13 and the hinge mutants retain high levels of BLA enzyme activity and maltose-binding affinity suggests that the BLA domain and MBP domain in these switches are structurally very similar to BLA and MBP. Since the I329W/A96W double mutation in MBP is known to cause the apo form of MBP to be almost all the way closed [11], we speculate that the apo forms of I329D and I329H are also almost fully closed. Interestingly, the I329K mutation improves switching with CFTX as substrate by threefold primarily through compromising  $k_{\text{cat}}$  in the absence of maltose. This further establishes the connectivity between the state of the MBP domain and the catalytic activity of the BLA domain.

Overall, the extent of switching appears to be a complex function of the properties of the amino acid at position 329, but with a distinct relationship to maltose affinity. We speculate that this relationship results from the dependence of maltose affinity and switching activity on the conformation of the MBP domain. The results with NCF and CFTX as substrate were qualitatively similar with a threshold value for the  $K_{\text{d}}$  for maltose of 0.5 μM below which switching activity was markedly worse. Marvin and Hellinga [10] demonstrated that mutations in the hinge region can improve the affinity of MBP for maltose. Their proposal that the further the hinge mutations close the apo-MBP, the higher the affinity for maltose was later confirmed by NMR studies [11]. If our mutants have increased maltose affinity for the same reason, the results suggest that for RG13 there is a threshold angle of closure past which RG13’s defect in catalytic activity in the absence of maltose is largely overcome.

#### Mutations selected for disrupting switching also increase affinity for maltose

Mutations that disrupt switching but do not impair catalytic activity would be useful in elucidating the mechanism by which switching occurs. As RG13 is compromised in

catalytic activity in the absence of maltose, *E. coli* cells expressing RG13 can grow at 256 μg/mL ampicillin only if maltose is supplemented to the media. A mutation that alleviated the defect in catalytic activity in the absence of maltose would allow the *E. coli* to grow at this concentration. We created an error-prone PCR library of RG13 and subjected this library to selection under these conditions to identify such mutations.

A library of  $\sim 10^6$  transformants was constructed by error-prone PCR under conditions that create, on average, one non-synonymous mutation per gene. This library was plated on LB plates containing 256 μg/mL ampicillin but lacking maltose. Colonies that formed were further screened in 96-well format for a loss of maltose dependence on BLA activity using NCF hydrolysis. We identified two independent mutants (A301T and A319T) that cause the catalytic rate to have a much smaller dependence on maltose compared to RG13. Kinetic characterization of purified protein showed that the decrease in switching results from an increase in catalytic activity in the absence of maltose (Table 3). Surprisingly, both mutations substantially increased the affinity of RG13 for maltose (Table 3). Their relationship between maltose affinity and switching activity matches that of the I329 mutants (Fig. 2B) suggesting that similar phenomena underlie the properties of both sets of mutations. Both A310 and A319 are located in or near the hinge region (Fig. 1). A301T, which increases the affinity for maltose almost 100-fold, is oriented pointing into the hinge region and the introduction of a larger, polar amino acid at this position may force the apo form of RG13 to be more closed, much as mutations at I329 are known to function. A319 is on a helix near the hinge region, the same helix in which BLA is inserted (BLA is inserted in place of residue 317).

#### Effect of maltose on the relative rates of acylation and deacylation

Penicillin and cephalosporin hydrolysis by BLA is well known to follow Scheme 1.

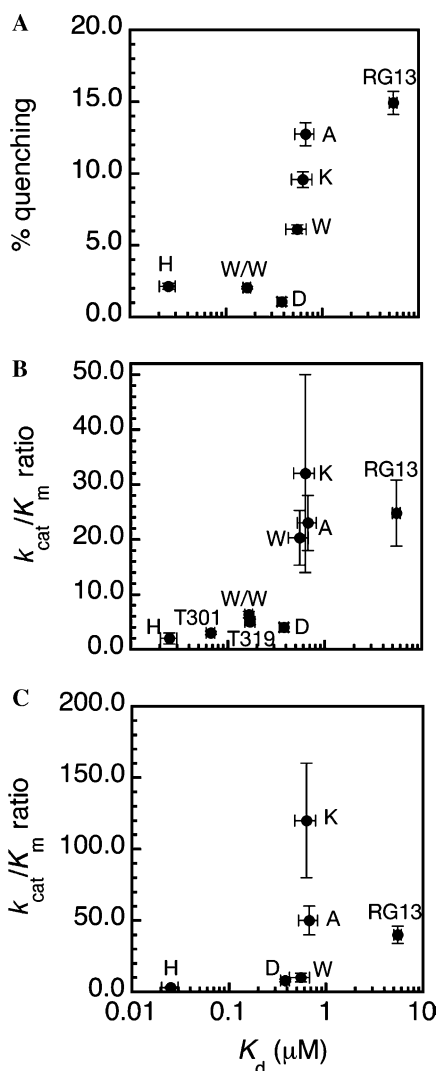


Fig. 2. Relationship between maltose affinity and other switch properties. (A) Percent intrinsic fluorescence quenching upon maltose binding as a function of the dissociation constant for maltose. Switching activity,  $(k_{\text{cat,mal}}/K_{\text{m,mal}})/(k_{\text{cat,0}}/K_{\text{m,0}})$ , with both nitrocefin (B) and cefotaxime (C) as substrates varies in a similar manner. Each switch is identified by the amino acid substituted at position 329 (i.e., 'A' refers to the I329A mutant). 'W/W' is the I329W/A96W double mutant. T301 and T319 are the A301T and A319T mutants identified in the genetic selection experiments.

Table 2  
Kinetic parameters of cefotaxime hydrolysis of RG13 and mutants in the presence and absence of maltose

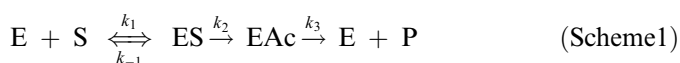
	RG13	I329W	I329P	I329A	I329D	I329K	I329H
$k_{\text{cat,mal}} (\text{s}^{-1})$	12 ± 3	9 ± 3	8 ± 1	8 ± 2	1.3 ± 0.3	15 ± 5	2.5 ± 0.7
$k_{\text{cat,0}} (\text{s}^{-1})$	1.1 ± 0.2	4 ± 1	0.7 ± 0.3	0.9 ± 0.2	0.3 ± 0.04	0.4 ± 0.1	1.0 ± 0.3
$k_{\text{cat,mal}}/k_{\text{cat,0}}$	11 ± 3	2 ± 1	11 ± 1	9 ± 3	4 ± 1	38 ± 15	3 ± 1
$K_{\text{m,mal}} (\text{mM})$	14 ± 3	9 ± 3	15 ± 2	9 ± 2	5 ± 1	17 ± 5	5 ± 1
$K_{\text{m,0}} (\text{mM})$	52 ± 4	41 ± 4	32 ± 12	48 ± 5	9 ± 1	60 ± 10	5 ± 1
$K_{\text{m,0}}/K_{\text{m,mal}}$	3.7 ± 0.8	4.6 ± 1.6	2.1 ± 0.8	5.3 ± 1.3	1.8 ± 0.4	3.5 ± 1.2	1.0 ± 0.3
$k_{\text{cat,mal}}/K_{\text{m,mal}} (10^2 \text{ s}^{-1} \text{ mM}^{-1})$	86 ± 9	99 ± 11	50 ± 6	85 ± 9	26 ± 3	86 ± 15	50 ± 10
$k_{\text{cat,0}}/K_{\text{m,0}} (10^2 \text{ s}^{-1} \text{ mM}^{-1})$	2.2 ± 0.4	10 ± 3	2.3 ± 0.3	1.8 ± 0.4	3.2 ± 0.3	0.7 ± 0.2	20 ± 4
$(k_{\text{cat,mal}}/K_{\text{m,mal}})/(k_{\text{cat,0}}/K_{\text{m,0}})$	40 ± 6	10 ± 3	20 ± 2	50 ± 10	8 ± 1	120 ± 40	3 ± 0.6

Subscripts 'mal' and '0' represent assay conditions in the presence of 5 mM maltose and absence of maltose, respectively.

Table 3  
Dissociation constants for maltose and kinetic parameters of nitrocefin hydrolysis of A301T and A319T in the presence and absence of maltose

	A301T	A319T
$k_{\text{cat,mal}} (\text{s}^{-1})$	390 ± 40	520 ± 50
$k_{\text{cat,0}} (\text{s}^{-1})$	280 ± 30	330 ± 40
$k_{\text{cat,mal}}/k_{\text{cat,0}}$	1.4 ± 0.1	1.6 ± 0.1
$K_{\text{m,mal}} (\mu\text{M})$	37 ± 3	40 ± 3
$K_{\text{m,0}} (\mu\text{M})$	78 ± 6	140 ± 10
$K_{\text{m,0}}/K_{\text{m,mal}}$	2.1 ± 0.2	3.5 ± 0.4
$k_{\text{cat,mal}}/K_{\text{m,mal}} (\text{s}^{-1} \mu\text{M}^{-1})$	10.5 ± 1.4	13.0 ± 1.6
$k_{\text{cat,0}}/K_{\text{m,0}} (\text{s}^{-1} \mu\text{M}^{-1})$	3.6 ± 0.5	2.4 ± 0.3
$(k_{\text{cat,mal}}/K_{\text{m,mal}})/(k_{\text{cat,0}}/K_{\text{m,0}})$	3 ± 0.3	5 ± 0.5
$K_{\text{d}}$ for maltose ( $\mu\text{M}$ )	0.067 ± 0.007	0.17 ± 0.02

Subscripts 'mal' and '0' represent assay conditions in the presence of 5 mM maltose and absence of maltose, respectively.



where E, S, ES, EAc, and P represent enzyme, substrate, non-covalent enzyme–substrate complex, covalent enzyme–substrate acyl intermediate, and hydrolyzed product, respectively. The Michaelis–Menten kinetic parameters,  $k_{\text{cat}}$  and  $K_{\text{m}}$ , are composed of several rate constants:  $k_{\text{cat}} = k_2 k_3 / (k_2 + k_3)$ ,  $K_{\text{m}} = K_s k_3 / (k_2 + k_3)$ , and  $K_s = (k_{-1} + k_2) / k_1$ .

Knowledge of the extent to which individual rate constants are affected by maltose would contribute to an understanding of the mechanism by which switching is occurring. However, RG13 in the absence of maltose exhibits a slight lag in the initial rate that is consistent with a hysteretic effect and not substrate inhibition [5]. This precludes the possibility of using stopped-flow methodologies for determining the individual rate constants. Instead, we addressed the relative rates of acylation ( $k_2$ ) and deacylation ( $k_3$ ) using hydroxylamine as an alternate nucleophile for the deacylation step. Several kinetic studies indicate that water is the nucleophile attacking EAc in the deacylation step [16]. The presence of a nucleophile stronger than water, such as hydroxylamine, will accelerate  $k_3$  and results in a covalently modified product [17,18]. Thus, if  $k_2 \geq k_3$ , hydroxylamine will increase the reaction velocity.

However, if  $k_2 \ll k_3$ , then hydroxylamine will have no effect on the reaction velocity.

If hydroxylamine participates as the nucleophile in the reaction, the product of NCF hydrolysis will be modified. Experiments were performed in which NCF was added to a solution containing the switch and 40 mM hydroxylamine and the reaction was allowed to progress until completion. The amount of switch added was sufficiently high such that the amount of product created from background hydrolysis of NCF by hydroxylamine alone was  $<1\%$  of the total NCF converted to product. Ethylacetate extraction was performed on the reaction mixture. We reasoned that the hydroxylamine-modified NCF product might possess a different partition ratio between ethylacetate and water than the product of NCF hydrolysis produced with water as the nucleophile. In the presence of hydroxylamine,  $35 \pm 7\%$  of the product partitions into the ethylacetate, but only  $10 \pm 3\%$  does so in the absence of hydroxylamine. This partitioning was independent of the presence of maltose. To confirm that hydroxylamine was not modifying the product after the reaction was complete, hydroxylamine was added after enzymatic hydrolysis. The amount of product partitioning into ethylacetate was  $11 \pm 2\%$  and independent of whether maltose was present, the same partitioning observed as in the absence of hydroxylamine. The hydroxylamine-modified NCF exhibited the same molar extinction coefficient at 486 nm as NCF hydrolyzed in the absence of hydroxylamine, consistent with hydroxylamine reacting with the carbonyl group of the NCF  $\beta$ -lactam ring, as water does [16]. Thus, hydroxylamine modifies the product of the reaction, but only if present during the enzymatic catalysis and not if added after the reaction was complete.

We next measured the rates of NCF hydrolysis catalyzed by RG13, in the presence and absence of maltose, as a function of hydroxylamine concentration. Although for penicillin substrates, BLA has similar values for  $k_2$  and  $k_3$  [19,20], for cephalosporin CFTX,  $k_2 \ll k_3$  [20]. This difference has been attributed to differences between the structures of cephalosporins and penicillins [20]. Since NCF is a cephalosporin, it was anticipated that  $k_2$  would

be much less than  $k_3$  for hydrolysis of NCF by maltose-bound RG13, since RG13 in the presence of maltose has essentially the same activity on NCF as BLA. This was confirmed as hydroxylamine did not accelerate the rate of reaction in the presence of maltose (Fig. 3A), indicating that  $k_2 \ll k_3$ . In contrast, in the absence of maltose, the rate of hydrolysis catalyzed by RG13 linearly increased with hydroxylamine concentration, indicating that  $k_2 \geq k_3$  (Fig. 3A). This indicates that maltose modulates the rate of NCF hydrolysis in part by modulating the relative values of  $k_2$  and  $k_3$ . The simplest and most likely explanation is that  $k_3$  is compromised in the absence of maltose and that maltose addition relieves whatever constraints are limiting deacylation. There is a good agreement on a role of E166 of BLA in activating water to deacylate the acyl-enzyme intermediate (EAc in Scheme 1) [16]. The major effect of a E166N mutation is a substantial decrease in the rate of deacylation [21]. Similarly, penicillin-binding proteins, which also form a long-lived acyl-enzyme complex with BLA substrates, do not have an equivalent residue to E166 [22]. We speculate that in the absence of maltose E166 in the BLA domain of RG13 may be subtly displaced resulting in a slower deacylation rate, and that this defect is alleviated by maltose-induced conformational changes.

We performed an identical analysis with the I329K, I329D (Figs. 3B and C), and I329P (not shown) mutants. The results with I329K and I329P were analogous to RG13, as might be expected since they all have similar switching activity. I329D exhibited a slight increase in rate with increasing hydroxylamine concentration in the presence of maltose and very little change, if any, in the absence of maltose. This is consistent with the fact that I329D is less compromised in the absence of maltose and is a poor switch. Hydroxylamine's small effect on the rate of NCF hydrolysis in the presence of maltose may reflect the fact that the I329D mutant is the most compromised mutant in terms of activity in the presence of maltose (i.e., the I329D mutant may be compromised in deacylation activity such that it has a higher  $k_2/k_3$  ratio than the other mutants in the presence of maltose). For I329D, the hydroxylamine

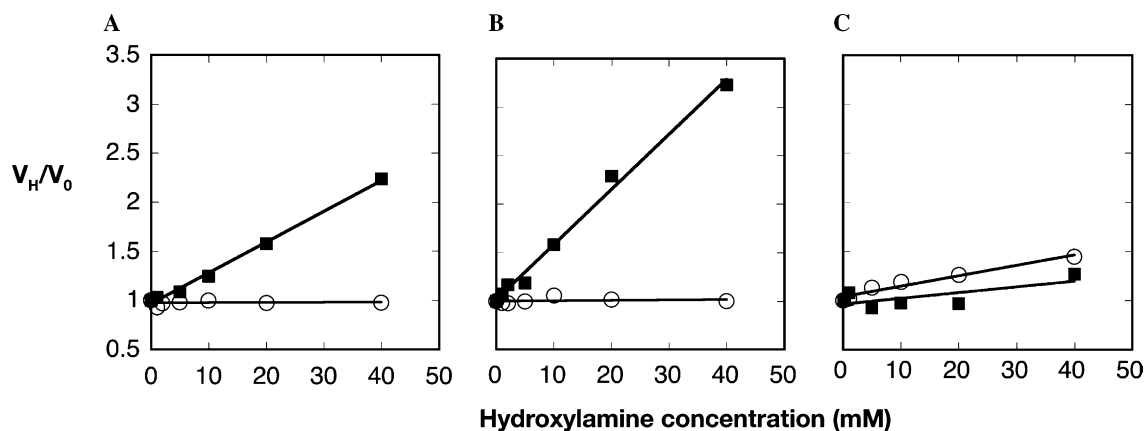


Fig. 3. Effect of hydroxylamine on nitrocefin (NCF) hydrolysis catalyzed by RG13 (A), I329K (B), and I329D (C) in the presence (empty circle) and absence (filled square) of 5 mM maltose.  $V_H$  and  $V_0$  represent NCF hydrolysis rate with and without 40 mM hydroxylamine, respectively.

experiments do not provide clear information about whether the relative rates of acylation and deacylation are changing upon maltose binding; however, either  $k_2$  or  $k_3$  or both must change since maltose binding increases  $k_{\text{cat}}$  threefold.

## Conclusions

The results suggest the following model for RG13 switching with NCF as the substrate. In the presence of bound maltose, the BLA domain of RG13 is in a conformation much like that of BLA and the rate-limiting step in catalysis is the formation of the acyl intermediate. In the absence of maltose, the BLA domain is in a conformation that is compromised in terms of the chemical steps. This conformation is also likely to be compromised as far as NCF binding since the absence of maltose has a negative effect on RG13's affinity for the substrate carbenicillin [5]. Unlike in the maltose-bound state, the rate of deacylation for the apo-form of RG13 is comparable to or less than the rate of acylation. The most likely explanation is that deacylation is compromised in the absence of maltose, perhaps because of a sub-optimal positioning of E166 of the BLA domain.

Studies on the hinge mutants provide information on what might be happening between the maltose-bound and maltose-unbound states of RG13. The correlation between maltose-induced quenching and switching activity, their relationship to maltose-affinity (Fig. 2), and the relationship between maltose affinity and apo-MBP's conformation all implicate the MBP domain's conformational change upon maltose binding in the switching activity. More specifically, the sharpness of the drop-off in switching activity as maltose affinity increases (a drop-off which results from an increase in catalytic activity in the absence of maltose) suggests that there exists a threshold conformation between the open and closed conformation. This hypothetical threshold conformation would exist at the angle closure at which the defect in NCF hydrolysis observed in apo-RG13 is largely alleviated (as the MBP domain progresses from the open to the closed conformation).

## Acknowledgment

This work was supported by a grant from NIH.

## References

- [1] C.A. Brennan, K. Christianson, M.A. La Fleur, W. Mandecki, Proc. Natl. Acad. Sci. USA 92 (1995) 5783–5787.
- [2] A. Villaverde, FEBS Lett. 554 (2003) 169–172.
- [3] D. Legendre, P. Soumillion, J. Fastrez, Nat. Biotechnol. 17 (1999) 67–72.
- [4] M. Ostermeier, Protein Eng. Des. Sel. 18 (2005) 359–364.
- [5] G. Guntas, S.F. Mitchell, M. Ostermeier, Chem. Biol. 11 (2004) 1483–1487.
- [6] G. Guntas, T. Mansell, J.R. Kim, M. Ostermeier, Proc. Natl. Acad. Sci. USA 102 (2005) 11224–11229.
- [7] A.J. Sharff, L.E. Rodseth, J.C. Spurlino, F.A. Quijcho, Biochemistry 31 (1992) 10657–10663.
- [8] F.A. Quijcho, J.C. Spurlino, L.E. Rodseth, Structure 5 (1997) 997–1015.
- [9] J.A. Hall, K. Gehring, H. Nikaido, J. Biol. Chem. 272 (1997) 17605–17609.
- [10] J.S. Marvin, H.W. Hellenga, Nat. Struct. Biol. 8 (2001) 795–798.
- [11] O. Millet, R.P. Hudson, L.E. Kay, Proc. Natl. Acad. Sci. USA 100 (2003) 12700–12705.
- [12] S.C. Gill, P.H. von Hippel, Anal. Biochem. 182 (1989) 319–326.
- [13] C. Moali, C. Anne, J. Lamotte-Brasseur, S. Gros Lambert, B. Devreese, J. Van Beeumen, M. Galleni, J.M. Frere, Chem. Biol. 10 (2003) 319–329.
- [14] G. Guntas, M. Ostermeier, J. Mol. Biol. 336 (2004) 263–273.
- [15] D. Paschon, M. Ostermeier, Methods Enzymol. 388 (2004) 103–116.
- [16] M. Oliva, O. Dideberg, M.J. Field, Proteins 53 (2003) 88–100.
- [17] Z. Wang, W. Fast, S.J. Benkovic, Biochemistry 38 (1999) 10013–10023.
- [18] Y.S. Simanenko, A.F. Popov, T.M. Prokop'eva, E.A. Karpichev, V.A. Savelova, I.P. Suprun, C.A. Bunton, Russ. J. Org. Chem. 38 (2002) 1286–1298.
- [19] H. Christensen, M.T. Martin, S.G. Waley, Biochem. J. 266 (1990) 853–861.
- [20] I. Saves, O. Burlet-Schiltz, L. Maveyraud, J.P. Samama, J.C. Prome, J.M. Masson, Biochemistry 34 (1995) 11660–11667.
- [21] G. Guillaume, M. Vanhove, J. Lamotte-Brasseur, P. Ledent, M. Jamin, B. Joris, J.M. Frere, J. Biol. Chem. 272 (1997) 5438–5444.
- [22] E. Gordon, N. Mouz, E. Duee, O. Dideberg, J. Mol. Biol. 299 (2000) 477–485.